# Topics in Oxy-Coal Retrofit of Utility Boilers – Burner Principles and Fire-Side Corrosion

Paper # 125

Andrew Fry*, Brad Adams, Kevin Davis, Marc Cremer, Dave Swensen, Shawn Munson
Reaction Engineering International
fry@reaction-eng.com
801 364 6925 x21
77 West 200 South, Suite 210
Salt Lake City, Utah 84101

Paul Kazalski
Siemens Environmental Systems & Services
paul.kazalski@siemens.com
908 470 3580
271 Route 202/206 PO Box 410
Pluckemin NJ, 07978

William Cox
Corrosion Management Ltd.
cox@corr-man.com
44 0 1788816231
21 Sedlescombe Park, Rugby
CV22 6HL United Kingdom

## ABSTRACT

Application of oxy-firing to existing power plants presents unquantified challenges as the characteristics of oxy-firing compared to air-firing have not yet been fully determined. Among the outstanding issues are the operation of oxy-coal burners and firing system within an air-fired utility boiler and fireside corrosion of waterwall and superheat tube metal surfaces. Results are presented from an experimental program where a 1.2 MW oxy-coal research burner was fired under air and oxy conditions in a pilot-scale furnace. The dependence of flame characteristics on primary velocity, $O_2$ concentration and mixing strategy are evaluated by evaluating flame shape and stabilization location. Ignition delay in oxy-coal flames was overcome by a 13% reduction in primary velocity. A stable and attached flame was achieved with no oxygen enrichment of the coal carrying gas. Oxygen injection at the burner face was most effective when introduced on the boundary between the primary and inner secondary gas streams. The corrosion rates of materials typical of coal-fired US utility boilers have been measured through implementation of a real-time electrochemical noise sensing technique for both air- and oxy-fired conditions. Materials chosen for this investigation include SA210 for the waterwalls and T22, P91 and 347H for the superheater. Waterwall corrosion rates decreased when converting from air to oxy-firing for all coals. Superheater corrosion rates increased when converting from air- to oxy-firing for most conditions tested. Corrosion rates for the lower alloyed materials (SA210 and T22) were shown to increase drastically during transients from reducing to oxidizing conditions when air-

firing and from oxidizing to reducing conditions when oxy-firing. The presence of trisulphates strongly increases the corrosion rate of the 347H material under high sulfur and low temperature conditions.

## INTRODUCTION

Future use of coal for power generation in the US depends on technologies being made available to capture and store $CO_2$ emissions from power plants. A key candidate $CO_2$ capture technology is oxy-firing of coal. Application of oxy-firing to existing power plants presents unquantified challenges as the characteristics of oxy-firing compared to air-firing have not been fully determined. Two key aspects of conversion to oxy-coal firing are 1) the impacts of oxygen injection and $CO_2$ flue gas recycle on burner feed design and resulting flame characteristics and 2) the impacts of oxy-coal firing on corrosion of boiler heat transfer surfaces.

Oxy-fuel burners are commonplace in high-temperature industrial furnaces today. Applications of oxy-fuel burners include: glass melting furnaces, electric arc furnaces, steel scrap melting, reheat and forging furnaces, soaking pit furnaces, ladle furnaces, aluminum melting furnaces, copper smelting and anode furnaces, hazardous waste incinerators, rotary enamel frit furnaces and lead melting furnaces. Some motivating factors for use of oxy-fuel burners include: high flame temperature and heat transfer, fuel savings, increase in production, pollutant reduction and reduction in capital cost.[1] Although the use of oxygen in burners is commonplace in industry today, oxy-coal burners for application in utility boilers are an emerging technology. Their application in typical steam generation boilers requires design considerations beyond our current experience. Consequently there is no established, or widely accepted, design methodology for burners of this type. Results presented here will focus on combustion and burner principles that will influence oxy-coal burner design and how they may differ from air-coal burner design considerations.

Since fire side water tube and steam tube corrosion was first recognized in the late 1950s, this problem has been the subject of many studies to identify mechanisms and to control corrosion propensities.[2,3] As a result of these studies, the number of fire-side corrosion problems has been reduced. However the problem has not been solved but just avoided by adjusting operating parameters such as steam temperature. It has also been reported that no known tube material is free of corrosion.[4] Recently, interest in fire-side corrosion has re-emerged due to an unexpected increase in corrosion in the furnaces modified for low NOx operation. Additional interest has been generated by efforts to increase boiler efficiency using advanced combustion system such as ultra-supercritical boilers and, more recently, to assess boiler suitability for oxygen-firing combustion.

Fire-side corrosion, categorized here as high temperature corrosion of waterwall and superheater/reheater tubes, can occur through a combination of various physicochemical phenomena occurring near the tube metal surface. Several corrosion mechanisms have been identified as relevant in coal-fired boilers: oxidation, sulfidation, and chloridation. The acting corrosion mechanism depends on local environment, determined by various key parameters and can occur through one dominant mechanism or a combination of multiple mechanisms. These mechanisms have been developed for air-fired conditions. The local environment in a furnace retrofit for oxy-combustion is expected to be very different from air-fired boilers.

Therefore known corrosion mechanisms need to be re-visited and potentially revised to account for the modified environment. As a part of this effort, published research studies relevant to oxidation, sulfidation, chloridation, carburization, and the issues related to oxy-firing conditions have been summarized elsewhere.[5] In addition, experimental measurements of corrosion under oxy-firing conditions are needed to provide data on which to base any needed refinements or adjustments to established corrosion mechanisms.

This paper will provide results from portions of an on-going DOE-funded program to characterize and predict impacts of $CO_2$ flue gas recycle and burner feed design on flame characteristics (burnout, emissions and heat transfer), fouling, slagging, and corrosion, inherent in the retrofit of existing coal-fired boilers for oxy-coal combustion. Results presented here will focus on two aspects of this program – oxy-coal burner testing and boiler tube corrosion testing.

## EXPERIMENTAL SETUP

### Test Furnace

Oxy-coal burner tests and corrosion tests were conducted in a 3.5 MBtu/hr pilot-scale combustor (L1500) at the University of Utah. The L1500 is a PC-fired furnace that was designed to simulate combustion in low emission, pulverized coal-fired boilers. This unit has been used for many investigations of technologies for $NO_x$ and particulate control, including: staging, reburning, SNCR and burner development. The reaction zone of this furnace has a 3.2 foot, square cross section and is approximately 46 feet in length. The length is divided into 10 sections, each with various sampling and injection ports. The furnace is refractory lined, with cooling panels in the first four sections to maintain realistic boiler temperature profiles. Multiple ports are located in each of the reactor sections, allowing for numerous configurations of sampling, reagent injection and overfire air. The pilot-scale combustor is represented in Figure 1 with some of its features and sample locations detailed.

**Figure 1. University of Utah's 3.5 MBtu/hr pilot-scale pulverized coal furnace (L1500).**

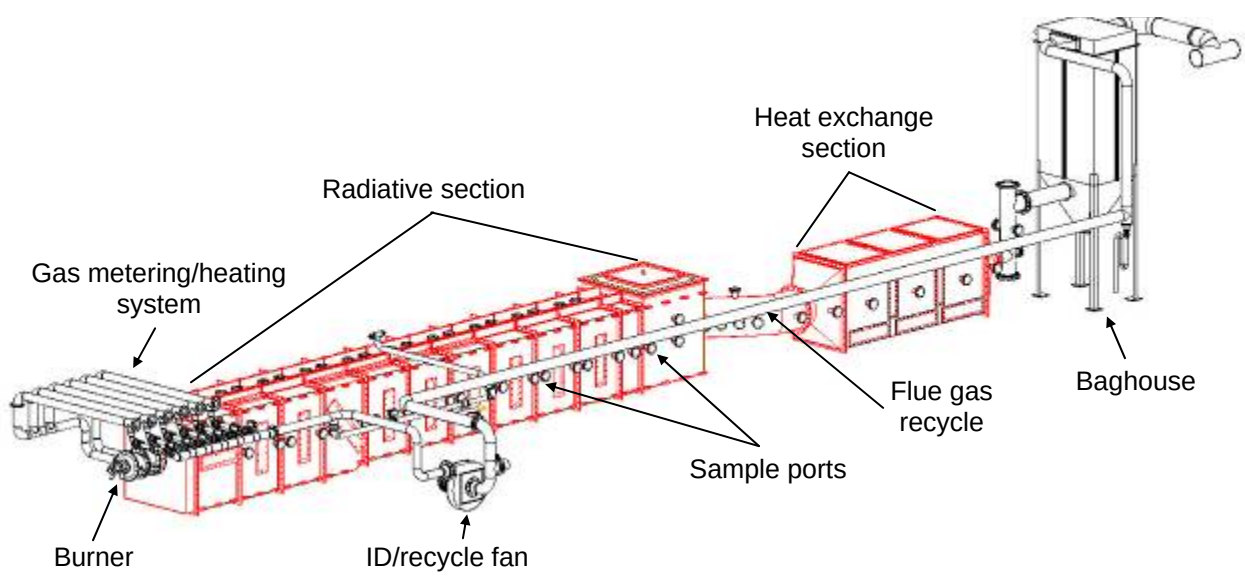

As detailed in Figure 1, the L1500 has been retrofit with a stainless steel pipe, fan and control system to allow recycle of flue gas back to the burner. These modifications, along with an $O_2$ and $CO_2$ supply and control system, make oxy-combustion experimentation possible.

The University of Utah has a Lenox FireSight 6545 high temperature camera for use in the L1500. This camera has been used to collect video detailing flame behavior for various air- and oxy-fired conditions. Figure 2 provides a diagram of the camera, the camera port in the burner plate and the camera viewing angle. The Lennox FireSight camera has a white cylindrical body which houses the temperature control equipment for the lens. The lens itself is mounted at the end of a stainless steel rod with the viewing angle of the lens orthogonal to the axis of the cylinder and rod. As depicted in Figure 2 the rod section of the camera is inserted through the port on the burner plate, pointing down the axis of the furnace. The depth of camera penetration is adjusted until the quarl exit is at the edge of the video frame and the view of the root of the flame is maximized. Still frame pictures produced with this camera configuration are presented in Figure 3.

**Figure 2. Description of camera configuration and field of view.**

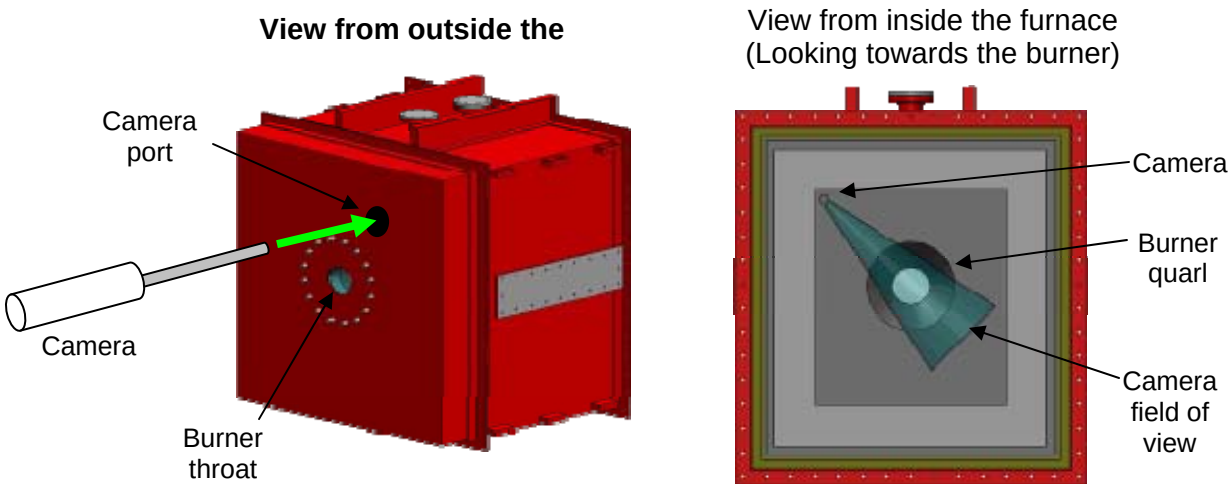


The still frame pictures in Figure 3 help to envision the orientation of the camera. However, the furnace sidewall and floor are opposite their expected location. This is because the camera inverts the picture left to right. This effect must be considered when interpreting video of the flame behavior. The exit of the burner quarl in the burner plate refractory can be seen in these pictures and is approximately 10 inches in diameter. The viewable area of the camera video extends approximately 15 inches downstream of the quarl exit.

**Figure 3. Still pictures from the camera with and without flame.**

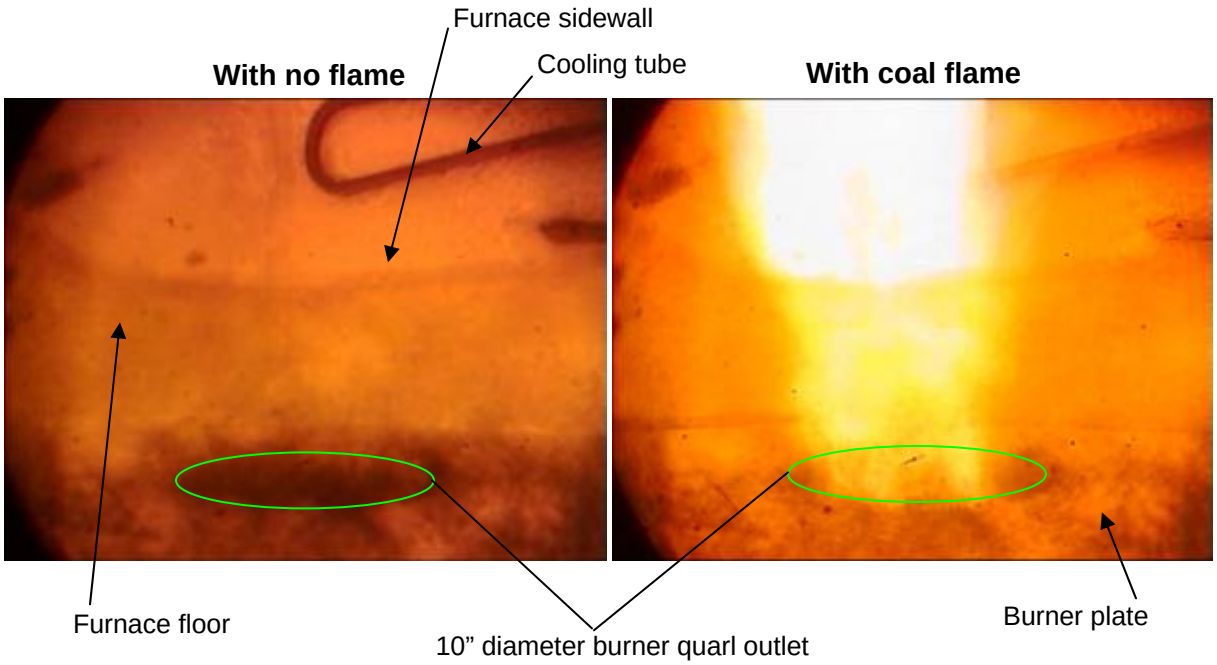


## Oxy-Coal Research Burner

For this program, the existing dual-register low-$NO_x$ burner on the L1500 was replaced with a 3.5 MBtu/hr oxy-coal research burner, designed jointly by Reaction Engineering International (REI) and Siemens Environmental Systems & Services (Siemens). The design of this burner was based on an existing Siemens oxy-burner design, but was modified to allow greater flexibility in the way that oxygen and flue gas recycle may be introduced and mixed in the near burner zone. This flexibility was necessary in order to facilitate research of various potential retrofit strategies of existing foal-fired utility boilers for oxy-combustion. Figure 4 shows a picture of the burner; more details of the burner configuration are presented elsewhere.[6]

**Figure 4. Oxy-coal research burner.**

The versatile design of the REI/Siemens oxy-coal research burner allows multiple configurations of introducing oxygen, coal and flue gas recycle (FGR), for optimization based on flame characteristics suitable for retrofit application (temperatures, stability, burnout, CO and $NO_x$). The purpose of the testing was not necessarily to optimize *this* particular burner for oxy-coal operation, but rather to develop *general principles* relevant to most wall-fired systems, with the oxy-research burner serving as but an example of how these general principles can be implemented in practice.

## Corrosion Measurement

Corrosion experiments were performed in the University of Utah's pilot-scale furnace utilizing electrochemical noise corrosion sensing technology, which yields real-time corrosion rate measurements. The principle of operation of this corrosion sensing technique is that spontaneous fluctuations in the measured electrical potential and current signals occur during corrosion. These fluctuations are monitored within an electrically isolated metal element and are subsequently converted to a real-time corrosion rate.[7] For these experiments one waterwall material and three superheat materials were chosen that are typical of US utility boilers. These materials were used for fabrication of corrosion elements in four distinct sensor probes. Specifications of the materials chosen are included in Table 1.

**Table 1. Specification of the materials used for corrosion sensor elements.**

| Material | SA 210 | T22 | P91 | 347h |
|---|---|---|---|---|
| HT Surface | Waterwall | Superheat | Superheat | Superheat |
| C, % | 0.07 | 0.11 | 0.10 | 0.048 |
| Si, % | 0.23 | 0.2 | 0.32 | 0.40 |
| Mn, % | 0.42 | 0.44 | 0.47 | 1.32 |
| Ni, % | - | - | 0.15 | 9.73 |
| Cr, % | - | 2.21 | 8.52 | 17.45 |
| Mo, % | - | 0.95 | 0.93 | - |
| S, % | 0.002 | 0.003 | 0.002 | 0.008 |
| P, % | 0.009 | 0.01 | 0.018 | 0.026 |
| Cu, % | - | - | 0.11 | - |
| Al, % | - | - | 0.01 | 0.005 |
| Nb/Cb, % | - | - | 0.07 | 0.63 |
| V, % | - | - | 0.22 | 0.078 |
| N, % | - | - | 0.044 | - |
| Ta, % | - | - | - | 0.02 |

The waterwall and superheat sensors differ in physical construction. The sensor elements on the waterwall probe are constructed from the SA210 material and are located at the tip of the probe on a face orthogonal to the probe axis. When installed in a furnace the probe is positioned so that the elements of the probe are in the same plane as the wall of the furnace. This configuration positions the corroding surface of the sensor elements as if they are a waterwall tube. The elements of the superheat probe are rings fabricated from actual boiler tube fabricated from T22, P91 and 347h. The corrosion surface of these elements has the tubing manufacturer's factory finish. These elements are situated at the end of a long, cooled stainless steel tube. When inserted into the furnace, the orientation of the sensor elements is that of a tube in cross flow, just like a superheat tube in a utility boiler. The corrosion sensor probe and furnace configuration for these tests is presented in Figure 5.

**Figure 5. Pilot-scale furnace and corrosion sensor probe configuration.**

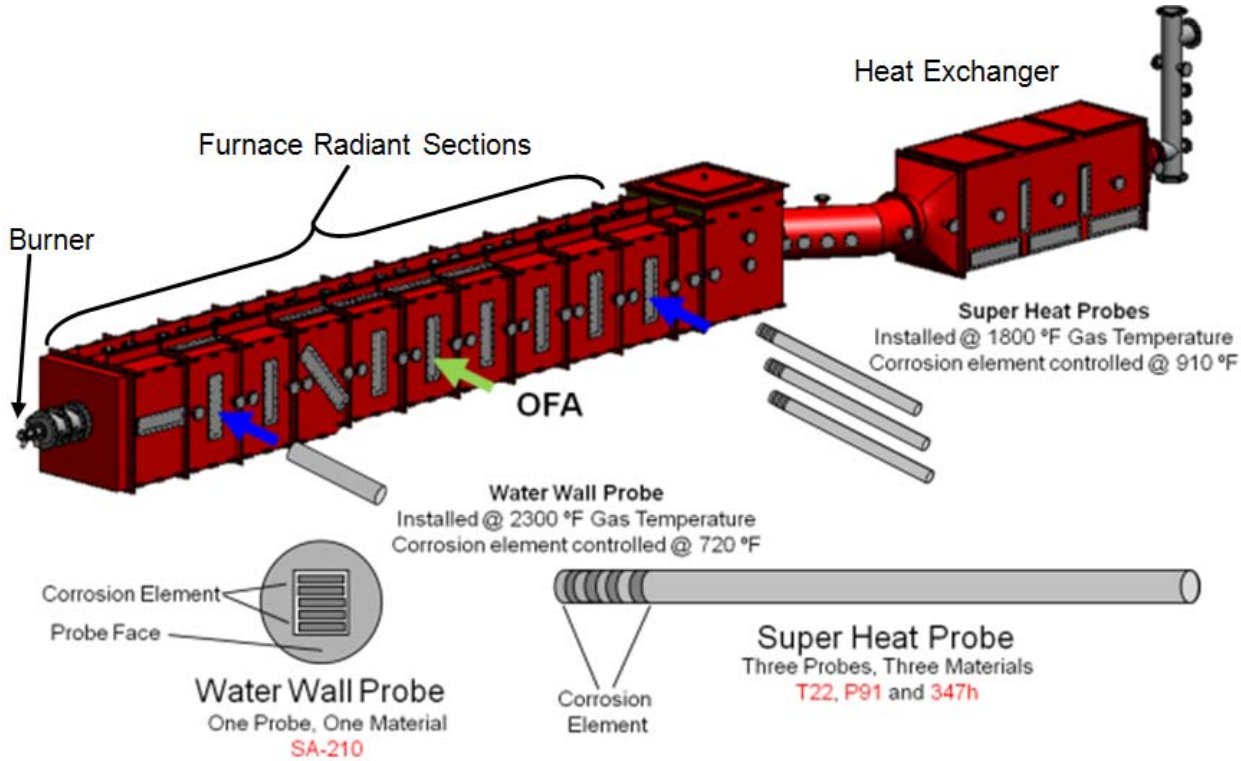


The sensor elements of the waterwall probe were typically maintained at 720 °F and the probe was installed in section 2 of the L1500 with gas temperatures about 2300 °F. The sensor elements on the superheat probes were typically controlled at 910 °F and were installed at a gas temperature of about 1800 °F. To target this gas temperature the superheat sensor probes were installed in section 10 of the L1500. For all fire-side corrosion tests, the firing rate was 3.5 MBtu. For the majority of these tests, the burner was staged with a stoichiometric ratio of 0.9. The overall stoichiometric ratio was sufficient to produce 3.0% $O_2$ (dry) in the flue gas and is dependent on air or oxy-fired conditions. The over-fire air was introduced in section 6 of the furnace. These will be referred to as the baseline conditions.

The average corrosion rates measured by this method assume that the metal loss occurs uniformly over the surface of the corrosion sensor element. In reality, the loss of material is more likely to occur in discrete locations on the sensor element associated with deposit and flow characteristics. For the superheater probes this discrete area is probably limited to about a third of the overall surface on the leading and trailing sides of the tube in cross flow. Peak corrosion rates therefore are likely to be approximately 3 times higher than the overall average rates reported here. However, as this is a pilot-scale facility which was operated only during an eight to ten hour period each day, and the corrosion probes were removed each night, the relative corrosion rate values were more relevant for comparison purposes than were the absolute rate values.

Three different coals were fired for these experiments, a western bituminous coal from the Utah Skyline mine, a high sulfur bituminous Illinois coal from the Shay #1 mine and a Powder River Basin (PRB) North Antelope coal. The Skyline coal was used for all of the burner and flame investigations and all three coals were used for the fire-side corrosion investigations. The properties of these coals are listed in Table 2.

**Table 2. Coal and mineral matter properties.**

| | Skyline | PRB | Illinois | | Skyline | PRB | Illinois |
|---|---|---|---|---|---|---|---|
| **Coal Analyses** | | | | **Mineral Matter Analyses** | | | |
| **C** | 70.60 | 53.72 | 64.67 | **Al** | 14.52 | 14.78 | 17.66 |
| **H** | 5.05 | 3.57 | 5.59 | **Ca** | 6.11 | 22.19 | 1.87 |
| **N** | 1.42 | 0.78 | 1.12 | **Fe** | 5.09 | 5.20 | 14.57 |
| **S** | 0.53 | 0.23 | 3.98 | **Mg** | 1.39 | 5.17 | 0.98 |
| **O** | 10.39 | 13.07 | 16.65 | **Mn** | 0.02 | 0.01 | 0.02 |
| **Ash** | 8.38 | 4.94 | 7.99 | **P** | 0.59 | 1.07 | 0.11 |
| **Moisture** | 3.18 | 23.69 | 9.65 | **K** | 0.57 | 0.35 | 2.26 |
| **Volatile Matter** | 38.60 | 33.36 | 36.78 | **Si** | 60.89 | 30.46 | 49.28 |
| **Fixed Carbon** | 49.39 | 38.01 | 45.58 | **Na** | 1.41 | 1.94 | 1.51 |
| **HHV, Btu/lb** | 12,606 | 9,078 | 11,598 | **S** | 2.33 | 8.83 | 2.22 |
| | | | | **Ti** | 0.88 | 1.30 | 0.85 |
| * all values in mass % unless otherwise specified | | | | | | | |

# RESULTS AND DISCUSSION

## Burner Principles

Experiments have been performed in the University of Utah's pilot-scale pulverized coal furnace using the oxy-coal research burner to evaluate flame behavior under air- and oxy-fired conditions. Particularly, oxy-fired conditions expected to be relevant for burner retrofit have been investigated. Video detailing the flame shape and stability along with furnace emissions for each of these conditions has been collected, providing insight into particular retrofit strategies.

Experiments have been performed directly comparing the flame shape and stabilization location for air-fired and oxy-fired conditions under a variety of potential oxy-fired operating strategies. One of these strategies was to operate with matched $O_2$ concentrations in the inner and outer registers of the secondary. This condition forfeits a degree of operating freedom at the burner. However, if $O_2$ can be mixed into the bulk secondary gas stream as opposed to independent controls for every secondary register of every burner, the amount and complexity of the equipment may be significantly reduced. Because of its potential importance for retrofit, this condition will be referred to as "Pseudo Air". "Pseudo Air" may be more appropriate to apply to a condition where the primary $O_2$ concentration was also matched with the two registers of the secondary, but this condition may not be attainable due to safety constraints in the burner primary register.

The conditions of the primary register of the burner have a strong influence on flame stabilization location due to particle heat up, devolatilization and ignition. Therefore consideration of primary operating conditions was one of the main focuses of this research. Matching the primary gas/fuel mass ratio, momentum and velocity with air-fired burner operation are some of the potential strategies for oxy-fired burner operation. Figure 6 provides a comparison of flame shape between an air-fired flame and an oxy-fired flame with a matched primary gas to fuel mass ratio and pseudo air in the secondary registers. The primary $O_2$ concentration is the same as the air-fired condition and the overall $O_2$ concentration in the $O_2$ FGR mixture is 27%.

**Figure 6. Comparison of air- and oxy-fired flames with a matched primary gas to fuel mass ratio.**

**Air-Fired**
BSR = 0.9
Air/Fuel = 1.8
IS/OS = 20/80

**Oxy-Fired**
Matched **Gas/Fuel Ratio**
BSR = 0.9
Primary Gas/Fuel = 1.80
IS/OS = 20/80
Primary $O_2$ Conc. = 21%
Primary SR = 0.162
Inner Secondary $O_2$ Conc. = 28.8%
Outer Secondary $O_2$ Conc. = 28.8%
Overall $O_2$ in $O_2$/FGR mixture = 27%

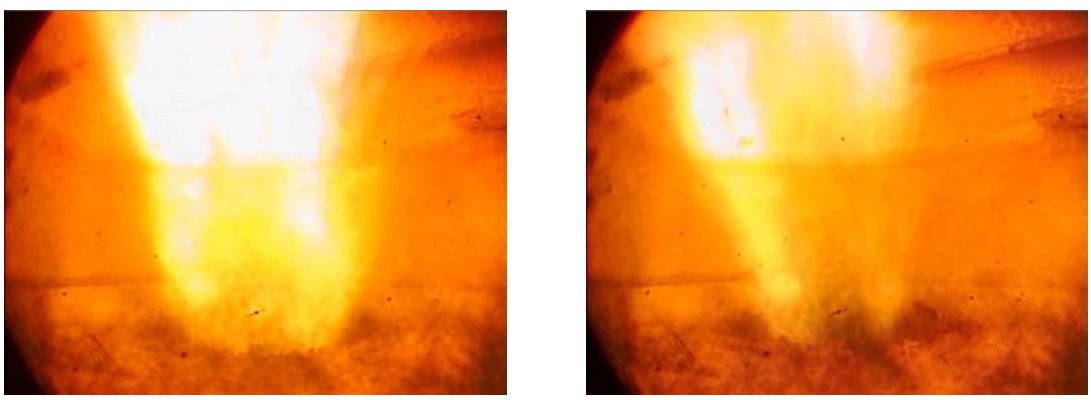

The oxy-fired conditions for this comparison were chosen to match heat transfer and not adiabatic flame temperature. Therefore the luminosity of the flame is expected to be lower for oxy-fired case than the air-fired case, due to the lower flame temperature. This was consistent with the pictures in Figure 6. The shape of the flame appeared to be similar for the oxy-fired and the air-fired cases. The ignition of the oxy-flame may have been somewhat delayed from the air case, but that was difficult to separate out from the lower luminosity. Oxy-fired conditions with a matched primary momentum to the air-fired case were also tested. These experiments yielded similar results to those shown in Figure 6. The oxy-fired flame was less luminous, but the flame was attached within the burner quarl.

The oxy-fired flame with a matched primary velocity to the air-fired conditions yielded different results. The flame for these conditions is compared with the air-fired flame in Figure 7.

**Figure 7. Comparison of air- and oxy-fired flames with a matched primary velocity.**

**Air-Fired**
BSR = 0.9
Air/Fuel = 1.8
IS/OS = 20/80

**Oxy-Fired**
Matched **Velocity**
BSR = 0.9
Primary Gas/Fuel = 2.0
IS/OS = 20/80
Primary $O_2$ Conc. = 21%
Primary SR = 0.179
Inner Secondary $O_2$ Conc. = 29.0%
Outer Secondary $O_2$ Conc. = 29.0%
Overall $O_2$ in $O_2$/FGR mixture = 27%

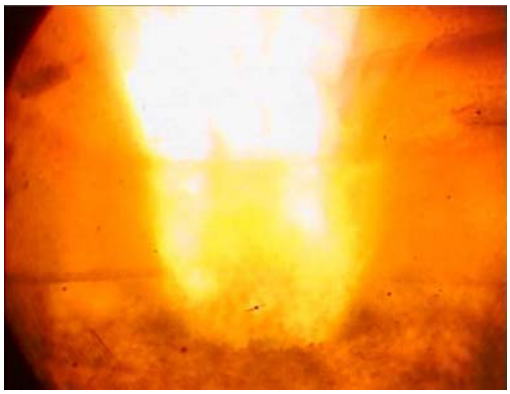

The behavior of the flames displayed in Figure 6 and Figure 7 indicate that there are fundamental differences between the ignition properties of an air and oxy-fired flame where ignition is delayed for the oxy-fired case. This phenomenon is likely due to the higher heat capacity of the coal carrier gases and lower flame temperatures and is discussed elsewhere.[8,9] These experiments indicate that the primary must be operated at a velocity approximately 13% lower than typical air-fired designs in order to compensate for delayed ignition. It is important to keep in mind that all three of these conditions provided a primary stoichiometric ratio that was lower than the air-fired condition, at 0.191. In order to match the stoichiometric ratio with the air-fired condition, the primary $O_2$ concentration would have needed to be raised significantly above 23.5% (a potentially unsafe condition) or the primary gas to fuel ratio would have to have been increased above 2.0. The latter condition had already been proven to result in a detached flame.

It has been theorized in the literature that due to safety constraints, it is unlikely that oxy-coal combustion will be performed in utility boilers with enrichment of oxygen in the coal-carrying gas.[10,11] This constraint would render the primary $O_2$ concentration equal to the flue gas exit $O_2$ concentration, about 3% dry. For this reason further experiments were targeted towards oxy-fired conditions with no primary $O_2$ enrichment. Figure 8 compares oxy-fired flames with the primary enriched to 21% $O_2$ and with only the recycled flue gas $O_2$ concentration.

**Figure 8. Comparison of two oxy-fired flames, one with primary $O_2$ enrichment and the other with no primary $O_2$ enrichment.**

**Oxy-Fired**
Matched **Gas/Fuel Ratio**
BSR = 0.9
Primary Gas/Fuel = 1.80
IS/OS = 20/80
Primary $O_2$ Conc. = **21.5%**
Primary SR = 0.162
Inner Secondary $O_2$ Conc. = 28.8%
Outer Secondary $O_2$ Conc. = 28.8%
Overall $O_2$ in $O_2$/FGR mixture = 27%

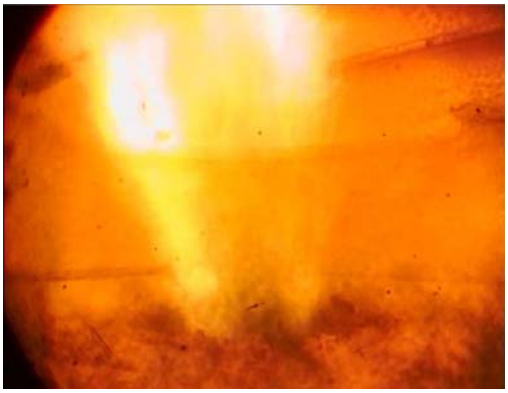

**Oxy-Fired**
**No Primary $O_2$ Enrichment**
BSR = 0.9
Primary Gas/Fuel = 1.80
IS/OS = 20/80
Primary $O_2$ Conc. = **2.7%**
Primary SR = 0.02
Inner Secondary $O_2$ Conc. = 34.5%
Outer Secondary $O_2$ Conc. = 34.5%
Overall $O_2$ in $O_2$/FGR mixture = 27%

The flame in Figure 8 with no primary $O_2$ enrichment has a flame that is well attached in the quarl. This indicates that the maximum velocity for flame attachment is probably not a function of primary $O_2$ concentration. However, the dark region in the center of the flame indicates that there was delayed ignition to a significant portion of the fuel for the low primary $O_2$ condition. These experiments show that it is possible to support an attached flame with low primary $O_2$ concentrations, but alternative methods of introducing oxygen may be necessary in order to maintain the flame shape and luminosity.

Experiments were performed to investigate the flame shape and stabilization location when removing oxygen from the primary and alternatively introducing it through injection lances at the burner face. These tests were performed while oxy-firing at conditions where the flame was flickering between being attached within the quarl and blown off. These conditions were chosen because there would be a clear indication of whether the injection strategy produced favorable or unfavorable results. To produce a flickering flame, the primary air to fuel ratio was set at 2.05, the inner/outer secondary mass ratio to 20/80, the primary $O_2$ concentration was 21% and pseudo air was used in the secondary register. The overall $O_2$ concentration in the $O_2$/FGR mixture was 27%. Figure 9 compares the baseline oxy-fired flame with a flame where the primary $O_2$ is injected axially into the primary through the bluff body.

**Figure 9. Comparison of a flame with no primary $O_2$ enrichment and primary $O_2$ injection with a flickering baseline flame.**

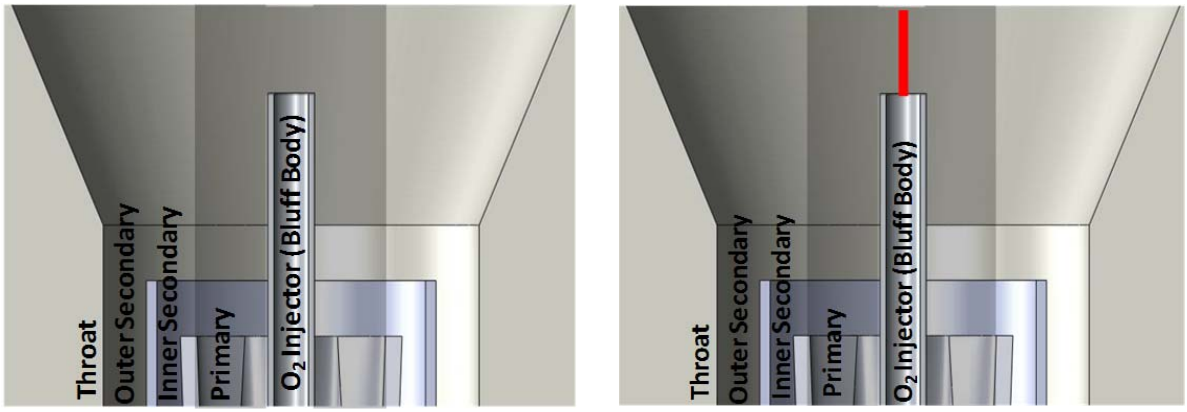


BSR = 0.9
Primary Gas/Fuel = 2.08
IS/OS = 20/80
Primary $O_2$ Conc. = 21.4% (Premixed)
Primary SR = 0.188
Inner Secondary $O_2$ Conc. = 29.8%
Outer Secondary $O_2$ Conc. = 29.2%
Overall $O_2$ in $O_2$/FGR mixture = 27%
**(Baseline)**

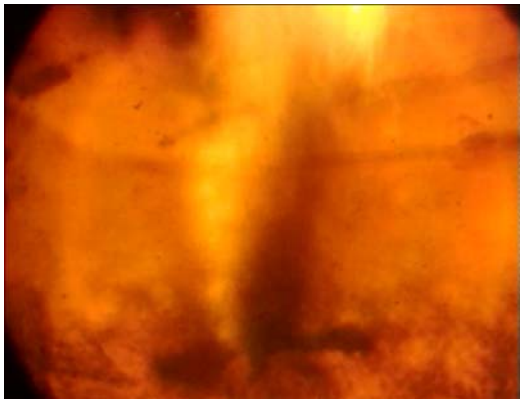

BSR = 0.9
Primary Gas/Fuel = 2.05
IS/OS = 20/80
**Primary $O_2$ Conc. = 2.46% (Premixed)**
**Primary SR = 0.018**
Inner Secondary $O_2$ Conc. = 38.1%
Outer Secondary $O_2$ Conc. = 29.5%
Overall $O_2$ in $O_2$/FGR mixture = 27%
**103 lb/hr $O_2$ (Axial Injection)**

The flames in Figure 9 indicate that the axial injection condition results in a detached flame, possibly more so than the baseline condition. This result should not be surprising. In the baseline condition the oxygen is uniformly distributed throughout the primary gases and in proximity to the coal. In the injected case the oxygen in concentrated in the center of the primary and introduced only at a point where ignition is expected. Similar experiments were performed where the primary $O_2$ was injected radially from the bluff body. The flame shape was altered by the radial momentum of the $O_2$, but the flame attachment location was not significantly affected.

Additional experiments were performed where the primary $O_2$ was injected through the inner secondary at the boundary between the primary and inner secondary gas flows. The results of this experiment are detailed in Figure 10.

**Figure 10. Comparison of a flame with no primary O2 enrichment and inner secondary O2 injection with a flickering baseline flame.**

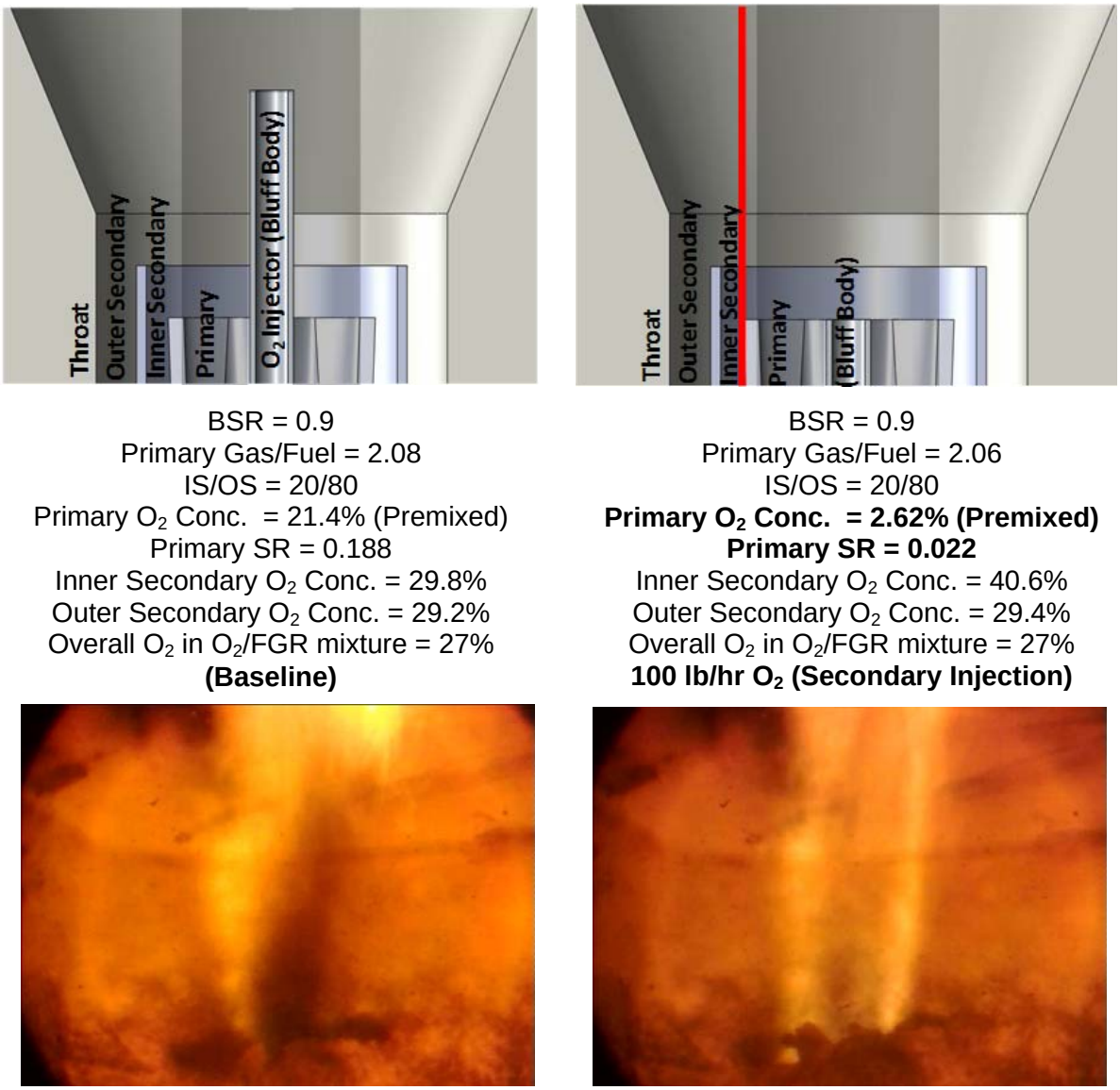


BSR = 0.9
Primary Gas/Fuel = 2.08
IS/OS = 20/80
Primary $O_2$ Conc. = 21.4% (Premixed)
Primary SR = 0.188
Inner Secondary $O_2$ Conc. = 29.8%
Outer Secondary $O_2$ Conc. = 29.2%
Overall $O_2$ in $O_2$/FGR mixture = 27%
**(Baseline)**

BSR = 0.9
Primary Gas/Fuel = 2.06
IS/OS = 20/80
**Primary $O_2$ Conc. = 2.62% (Premixed)**
**Primary SR = 0.022**
Inner Secondary $O_2$ Conc. = 40.6%
Outer Secondary $O_2$ Conc. = 29.4%
Overall $O_2$ in $O_2$/FGR mixture = 27%
**100 lb/hr $O_2$ (Secondary Injection)**

Figure 10 shows that when oxygen is injected through the nozzles in the inner secondary, the flame is strongly attached within the quarl. The overall results from the $O_2$ injection tests indicate that oxygen can be removed from the primary and introduced through injectors at the burner face and a stable flame can be achieved. However the location where the injection occurs is very critical to the flame stability. In our experiments, injection through the inner secondary was successful where injection into the primary through the bluff body was not. When $O_2$ is injected along the boundary between the inner secondary it is likely mixed rapidly with the coal-rich region. This mixing is motivated by shear between the primary and secondary gasses of differing velocity.

## Fire-Side Corrosion

REI and Corrosion Management Ltd. performed pilot-scale experiments to elucidate the potential impacts of oxy-coal combustion retrofit of utility boilers on heat transfer surface corrosion. The goals of these tests were two-fold:

1. To demonstrate differences, if any, in corrosion behavior of materials typically implemented in US utility boilers between air-coal and oxy-coal combustion conditions.
2. To develop a data set suitable for validation of mechanisms developed to predict the corrosion rate of heat transfer surfaces under air- and oxy-fired coal combustion conditions.

Over a period of six weeks of furnace operation, extensive measurements of the corrosion rates for each of the materials was performed at baseline conditions. These data were evaluated for windows in time where the furnace and probes were operating stably at the desired conditions. All of the data from these windows of operation were reduced to an average corrosion rate for every combination of material and coal. The average corrosion rates measured for the baseline conditions are presented in Figure 11 on two different scales.

**Figure 11. Summary of average corrosion rates for the baseline sensor element temperatures, probe locations and staging conditions (two scales).**

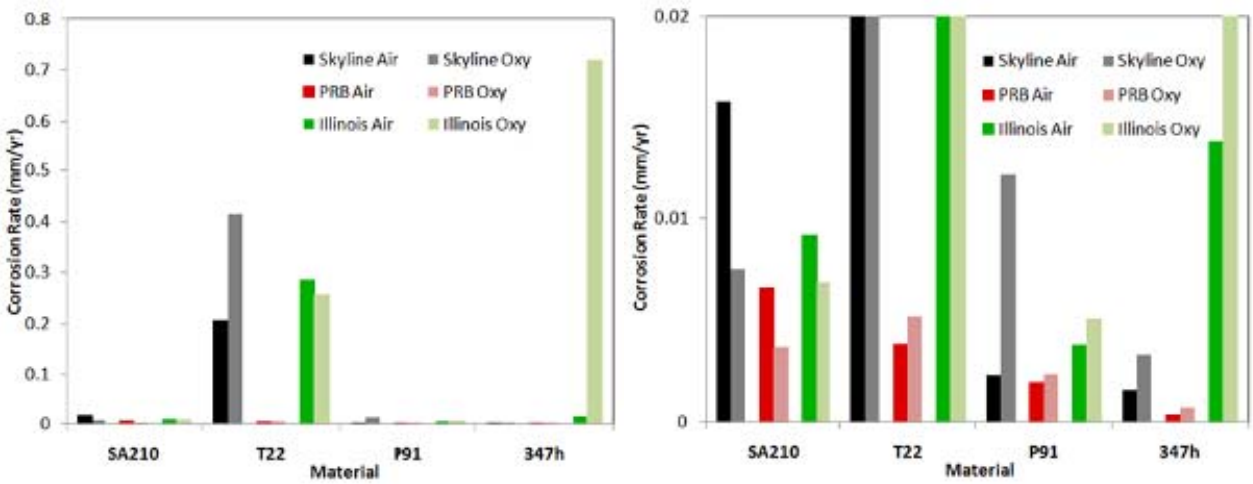


Figure 11 shows comparative rates under air and oxy fuel firing for each of the materials under test. Very low corrosion rates were evident for all of the materials, coals and air and oxy-firing, with the exception of five conditions. These conditions included the T22 material with Skyline and Illinois coals and for both air and oxy-fired conditions and the 347H material under Illinois/Oxy conditions. These five conditions and material combinations gave indicated rates on the order of 0.21 to 0.72 mm/yr (8.3 to 28.3 mils/year).

Corrosion rates of the remaining material and coal combinations range from 0.0034 to 0.016 mm/yr (0.13 to 0.62 mils/yr). Figure 11 details a significant trend between the air and oxy-fired conditions. For the waterwall probe (SA210), the corrosion rate decreased when the combustion conditions were changed from air- to oxy-firing for all conditions tested. By contrast, for all of

the superheater probes (T22, P91 and 347H) the corrosion rate increased when combustion conditions in the furnace were changed from air- to oxy-firing for all but one condition tested. To examine these trends in more detail it is useful to look at the plot of the increase in corrosion rate when converting from air- to oxy-firing for all materials and conditions. This plot is presented in Figure 12 on two scales.

**Figure 12. Measured increase in corrosion rate when converting from air- to oxy-firing (two scales).**

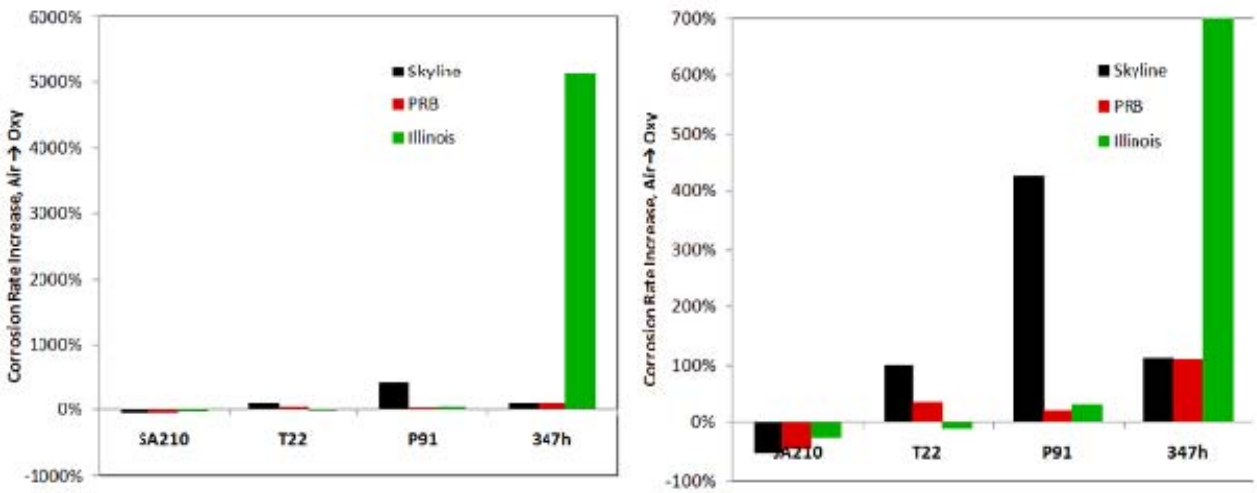


Figure 12 clearly indicates the difference in behavior between the waterwall and the superheater probes. The only material and coal that exhibited behavior that was contrary to the general trend was the T22 material with Illinois coal. The decrease in waterwall corrosion rate when converting from air to oxy-fired conditions, although involving minor corrosion rates, could be a significant circumstance. An expected decrease in corrosion rate to these heat transfer surfaces when retrofitting for oxy-combustion could be a facilitating result for the technology. The difference in behavior between the waterwall and superheater probes may be explained by the difference between oxidizing and reducing conditions. For these data, the waterwall probe was installed in a region with stoichiometry of 0.9, whereas the superheater probes experienced superstoichiometric conditions.

Additional experiments were performed to determine the effect of transitions between oxidizing and reducing conditions. For these experiments, the superheat probes were moved to section five of the furnace, just inside of the OFA ports. The burner stoichiometric ratio was varied between 0.9 and either 1.16 and 1.09 for air- and oxy-fired conditions respectively. The upper limit of the variation was designed to produce 3% $O_2$, dry, in the furnace exit flue gas. As the furnace was varied between staged and unstaged conditions, air, or $O_2$ and FGR, moved between the burner secondary and the air ports. A good indicator of transitions between staged and unstaged conditions was the flow rate of the outer secondary air register. This value along with superheater probe corrosion rates are plotted in Figure 13 for the staging experiments described above.

**Figure 13. Superheater probe corrosion rates for oxidizing and reducing conditions while oxy- and air-firing Illinois coal.**

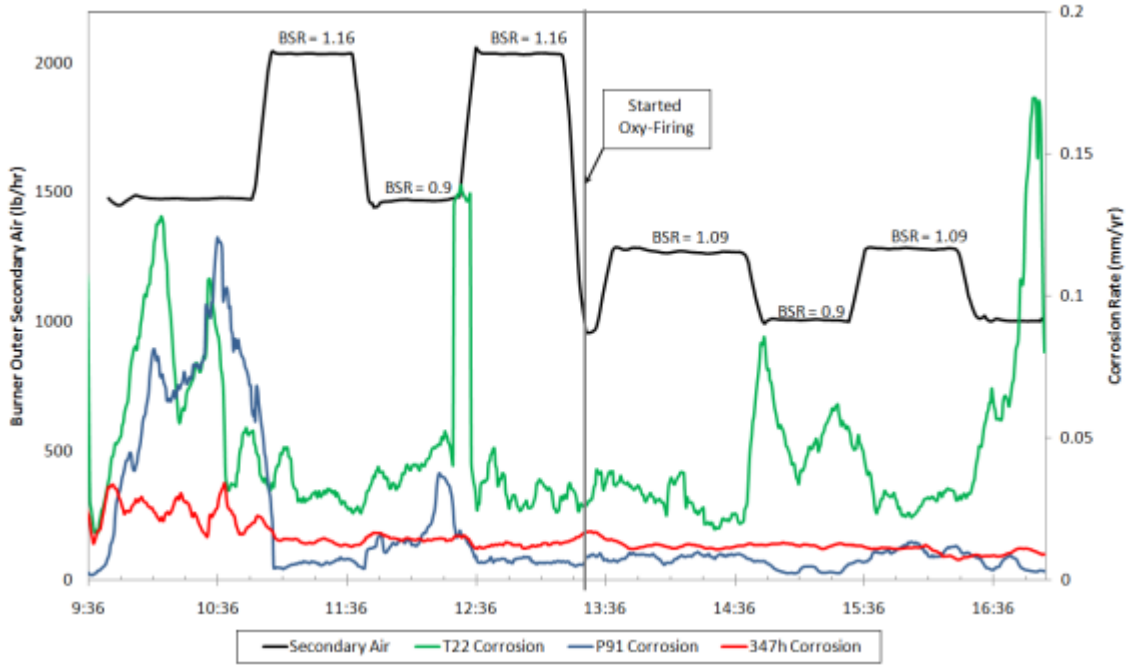


For the initial hour and a half, the corrosion rates seem to be coming to steady state after being installed in the furnace. This was probably because the deposit characteristics were different for this probe location and the surface condition on the probes required a longer-than-normal period to equilibrate to the new flue gas environment. During the first half of the day, air-fired conditions were tested. At this time, two variations from reducing to oxidizing operation were tested. The first variation occurred while the probes were still equilibrating. The second variation showed a strong impact on corrosion rate for the T22 material right as the conditions are varied from reducing to oxidizing.

For the second half of the day, oxy-fired conditions were tested. Conditions were varied from oxidizing to reducing two times. Under oxy-fired conditions, the T22 corrosion rate spiked during the transient from oxidizing to reducing conditions, which was the opposite behavior to that observed under the air-fired conditions. It appeared that the higher alloy materials were unaffected by transients between oxidizing and reducing conditions. Similar behavior was observed for the waterwall probe made of the SA 210 material. These results indicate that the corrosion rate of low-alloyed materials may be very high is regions of variable SR like in the near burner region and around OFA ports.

These are results that coupon tests with synthesized gas and deposits cannot resolve. The results are expected also to have a strong relationship to elevated corrosion rates in regions of fluctuating stoichiometry such as in the near-burner zone and around over-fire air ports. Data such as these can be used in advanced combustion modeling to develop and tune corrosion mechanisms for predicting accurately the impacts of fluctuations between oxidizing and reducing conditions.

Experiments were performed to determine the temperature dependence of the corrosion rates. For these experiments, the controlled temperature set points of the corrosion sensor elements were varied from their baseline condition up to the maximum operating temperature of the material. The upper temperature set points were 850, 1050, 1100 and 1300°F for the SA210, T22, P91 and 347H materials respectively. The first temperature variation experiment returned surprising results for the 347H material while oxy-firing Illinois coal. Immediately when the probe was heated, the corrosion rate dropped off. This behavior is depicted in Figure 14.

**Figure 14. Inverse temperature dependence of 347h superheat probe corrosion rate on temperature while oxy-firing Illinois coal.**

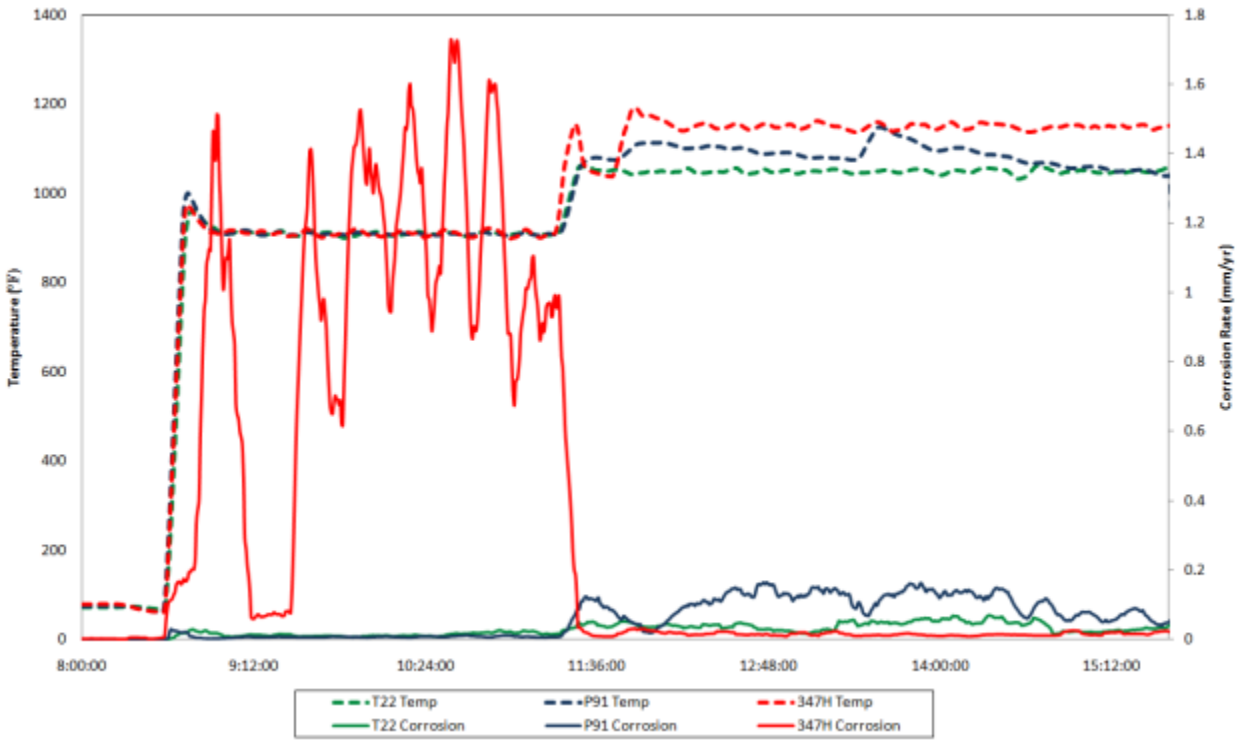


Figure 14 shows that at 11:23 the temperature set points of the corrosion elements were increased. As the temperature of the 347H probe increased, the corrosion rate began to fall dramatically, and it resumed a corrosion rate that was similar to that observed previously under the air-fired condition. It was concluded that this behavior was due to decomposition and volatilization of the trisulphate species.[12] This behavior may explain why the corrosion rate was so high for the 347H material while oxy-firing Illinois coal that was reported in Figure 11.

Further experiments to determine the dependence of corrosion rate on temperature were performed. Some of these data are presented in Figure 15.

**Figure 15. Plot showing the temperature dependence of the superheater corrosion probes while oxy-firing Illinois coal.**

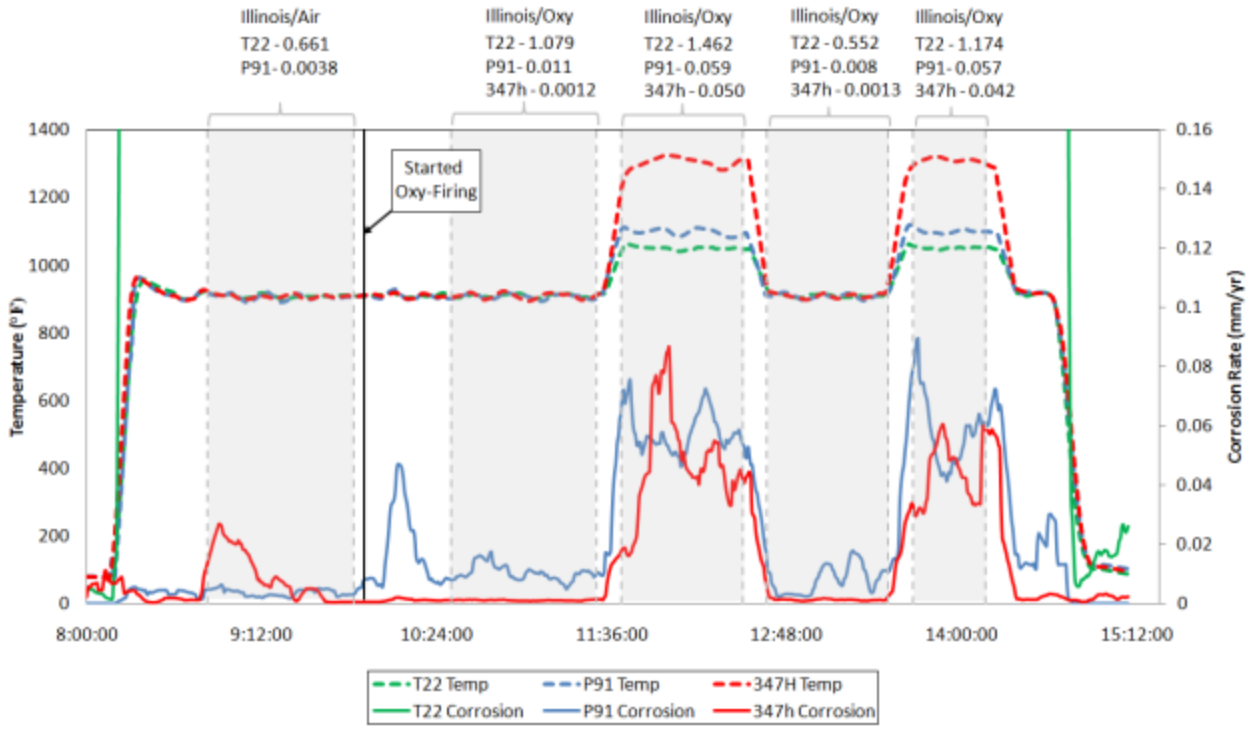


In Figure 15 the operating temperatures and corrosion rates of each of the superheat probes are presented. The gray areas on each plot indicate a time periods when the data were averaged and used in the overall average for that condition. The average values for each of the corrosion rates are also included at the top of each of the grey areas. These data not only indicate the temperature dependence of the data, but also demonstrate the excellent repeatability and consistence of the rate estimates.

## SUMMARY

An extensive test campaign has been performed in the University of Utah's pilot-scale pulverized coal furnace. These experiments were performed to characterize and predict impacts of $CO_2$ flue gas recycle and burner feed design on flame characteristics (burnout, emissions and heat transfer) and corrosion, inherent in the retrofit of existing coal-fired boilers for oxy-coal combustion.

Results from burner testing showed:

- Matching the primary gas/fuel mass ratio and matching the primary momentum with air-fired conditions both resulted in a flame stabilized within the quarl while operating with Pseudo Air in the secondary registers. Matching primary velocity with the air-fired conditions resulted in a blown off (detached) flame. These data indicated a fundamental difference in flame behavior between the air- and oxy-fired conditions with a delay in flame ignition for the oxy-fired conditions. A decrease in primary velocity of 13% was necessary in order to stabilize a flame within the quarl.

- A flame could be stabilized with no oxygen enrichment of the primary (3% $O_2$ in the primary) while using Pseudo Air in the secondary registers. However the luminosity of the flame was decreased, suggesting delayed ignition for much of the coal not on the boundary between the primary and inner secondary.
- Oxygen injection at the burner face was performed where the oxygen was introduced through lances within the primary and inner secondary registers. These tests were intended to provide an alternative to primary oxygen enrichment. In our experiments, injection through the inner secondary was successful where injection into the primary through the bluff body was not. When $O_2$ is injected along the boundary between the inner secondary it is likely mixed rapidly with the coal-rich region. This mixing is motivated by shear between the primary and secondary gasses of differing velocity.

Results from corrosion testing showed:

- For baseline conditions, the corrosion rates were in the ranges of 0.21 to 0.72 mm/yr (8.3 to 28.3 mils/year) for the T22 material with both Skyline and Illinois coals under air- and oxy-fired conditions and for the 347H probe when Illinois coal was oxy-fired the corrosion rates were in the range of 0.0034 to 0.016 mm/yr (0.13 to 0.62 mils/yr). These corrosion rates are assuming that the loss of material occurs evenly over the entire sensor element. Actual peak corrosion rates are expected to be on the order of 3 times higher. Waterwall corrosion rates decreased when converting from air to oxy-firing for all coals. Superheater corrosion rates increased when converting from air- to oxy-firing for all conditions with the exception of the T22 material when firing Illinois coal.
- Corrosion rates for the lower alloyed materials (SA210 and T22) were shown to increase drastically during transients from reducing to oxidizing conditions when air-firing and from oxidizing to reducing conditions when oxy-firing. Such transients are likely to contribute greatly to practical in-plant corrosion rates in the near-burner and near-OFA port regions. These effects cannot be resolved using coupon tests.
- The presence of trisulphates strongly increases the corrosion rate of the 347H material under high sulfur and low temperature conditions. It was demonstrated conclusively, (and for the first time by real-time corrosion monitoring, and in confirmation of published literature predictions) that these species are decomposed by operating at higher material temperatures, reducing the subsequent corrosion rates to much lower levels.
- The dependence of corrosion rate on material temperatures was demonstrated along with the repeatable nature of the results.

## ACKNOWLEDGMENTS

This material is based upon work supported by the Department of Energy under Award Number DE-NT0005288. Project Manager is Timothy Fout. This report was prepared as an account of work sponsored by an agency of the United States Government. Neither the United States Government nor any agency thereof, nor any of their employees, makes any warranty, express or implied, or assumes any legal liability or responsibility for the accuracy, completeness, or usefulness of any information, apparatus, product, or process disclosed, or represents that its use would not infringe privately owned rights. Reference herein to any specific commercial product, process, or service by trade name, trademark, manufacturer, or otherwise does not necessarily

constitute or imply its endorsement, recommendation, or favoring by the United States Government or any agency thereof. The views and opinions of authors expressed herein do not necessarily state or reflect those of the United States Government or any agency thereof.

## REFERENCES


1. Kobayashi H. and Tsiava R., "Oxy-Fuel Burners," in Baukal C E, *Industrial Burners Handbook*, New York, CRC Press, 693–723, 2004.

2. Harb JN, Smith EE, "Fireside Corrosion in Coal-Fired Boilers," Prog Energy Combust Sci 16, 169-190, 1990.

3. Raask E, "Mineral Impurities in Coal Combustion," Washington DC, Hemisphere Publishing, 1985.

4. Rehn IM, "Fireside corrosion of superheater alloys for advanced-cycel steam plants," EPRI Rep CS-5195, 1987.

5. Adams B R, Fry A R, Senior C L, Shim H S, Wang HF, Wendt J O L, Shaddix C, "Characterization of Oxy-combustion Impacts in Existing Coal-fired Boilers," DOE Topical Report, Cooperative Agreement DE-NT0005288, pp. 120-144, July 2009.

6. Fry, A., B. Adams, M. Cremer and J. Shan, "Development of Oxy-Burner Retrofit Principles for Existing Coal-Fired Utility Boilers," presented at the "1st IEA GHG, Oxy-Fuel Combustion Conference," Cottbus, Germany, Sept. 7-11, 2009.

7. Bakker, W. T., Mok, W. Y., and Cox, W. M., "High-Temperature Fireside Corrosion Monitoring in the Superheater Section of a Pulverised-Coal-Fired Boiler", EPRI, Palo Alto, CA: 1992, TR-101799.

8. Shaddix C R and Molina A (2009), 'Particle imaging of ignition and devolatilization of pulverized coal during oxy-fuel combustion', *Proc. Combust. Inst.*, 32, 1905–1912.

9. Khare S P, Wall T F, Farida A Z, Liu Y, Moghtaderi B and Gupta R P (2008), 'Factors influencing the ignition of flames from air-fired swirl pf burners retrofitted to oxy-fuel', *Fuel*, 87, 1042–1049.

10. Toftegaard M B, Brix J, Jensen P A, Glarborg P, Jensen A D (2010), 'Oxy-fuel combustion of solid fuels', *Prog Energy Combust Sci*, 36, 581–625.

11. Zanganeh K E and Shafeen A (2007), 'A novel process integration, optimization and design approach for large-scale implementation of oxy-fired coal power plants with CO2 capture', *Int J Greenhouse Gas Control*, 1, 47–54.

12. Viswanathan, R, and Bakker, W. T., "Materials for Boilers in Ultra Supercritical Power Plants", Proceedings of the International Joint Power Generation Conference, Miami Beach, Fl., July 23-26, 2000.



## KEY WORDS

Oxy-Combustion, Retrofit, Burner, Flame, Ignition, Corrosion